


ARTICLE

Caspase inhibition prolongs inflammation by promoting a signaling complex with activated RIPK1

Xinyue Huang, Shuixia Tan, Yanxia Li, Shuangyi Cao, Xingyan Li, Heling Pan, Bing Shan, Lihui Qian, and Junying Yuan 

Activation of inflammation by lipopolysaccharide (LPS) is an important innate immune response. Here we investigated the contribution of caspases to the LPS-mediated inflammatory response and discovered distinctive temporal roles of RIPK1 in mediating proinflammatory cytokine production when caspases are inhibited. We propose a biphasic model that differentiates the role of RIPK1 in early versus late phase. The early production of proinflammation cytokines stimulated by LPS with caspase inhibition is mediated by the NF- κ B pathway that requires the scaffold function of RIPK1 but is kinase independent. Autocrine production of TNF α in the late phase promotes the formation of a novel TNFR1-associated complex with activated RIPK1, FADD, caspase-8, and key mediators of NF- κ B signaling. The production of proinflammatory cytokines in the late phase can be blocked by RIPK1 kinase inhibitor Nec-1s. Our study demonstrates a mechanism by which the activation of RIPK1 promotes its own scaffold function to regulate the NF- κ B-mediated proinflammatory cytokine production that is negatively regulated by caspases to restrain inflammatory signaling.

Introduction

Receptor-interacting serine/threonine protein kinase 1 (RIPK1) is a master regulator of the cellular decision between pro-survival nuclear factor- κ B (NF- κ B) signaling and cell death in response to a broad set of inflammatory and prodeath stimuli in human diseases (Ofengeim and Yuan, 2013; Yuan et al., 2019). RIPK1 is a 76-kD protein that contains an N-terminal kinase domain, a C-terminal death domain (DD), and an intermediate domain with a receptor-interacting protein homotypic interacting motif. The scaffold function of RIPK1 is important for mediating prosurvival NF- κ B signaling; in contrast, the activation of RIPK1 kinase is known to be involved in mediating prodeath activities, including necroptosis, RIPK1-dependent apoptosis, and inflammation (Mifflin et al., 2020). Thus, it has been generally accepted that the scaffold of RIPK1 serves a prosurvival function by promoting NF- κ B activation, which is opposite to its prodeath kinase activity. However, it remains unclear if and how the activated RIPK1 may regulate its scaffold function in dictating distinct cellular responses.

Caspases are important regulators of RIPK1 kinase (Yuan et al., 2016). Activation of death receptors by their cognate ligands with caspase inhibition promotes necroptosis, a form of regulated necrotic cell death mechanism mediated by RIPK1 kinase and its downstream mediators, including RIPK3 and MLKL (Shan et al., 2018; Wallach et al., 2016). Caspase-8-mediated cleavage after Asp324 in human RIPK1 (or Asp325

in murine RIPK1) is an important mechanism that negatively regulates the activation of RIPK1, as the cleavage separates the kinase domain in the N-terminal part of RIPK1 from its intermediate domain and DD, which is involved in mediating the activation of the N-terminal kinase by dimerization (Lin et al., 1999; Meng et al., 2018; Xu et al., 2018). Homozygous D325A mutation in murine *Ripk1* sensitizes cells to both apoptosis and necroptosis induced by TNF α and leads to embryonic lethality. The early demise of *Ripk1*^{D325A/D325A} mice can be rescued by simultaneous deletion of *Ripk3* and Fas-associated protein with DD (*Fadd*; Zhang et al., 2019) or of *Mlkl* and *Fadd* (Newton et al., 2019). Disrupted cleavage of RIPK1 by caspase-8 in humans leads to a dominantly inherited condition characterized by recurrent fevers with increased levels of proinflammatory cytokines and a strong RIPK1-dependent activation of inflammatory signaling pathways (Lalaoui et al., 2020; Tao et al., 2020). Consistently, the expression of RIPK1 D325V or D325H mutants in mouse embryonic fibroblasts also induces the expression of proinflammatory cytokines such as IL6 and TNF α . However, it remains unclear how blocking the caspase-mediated cleavage of RIPK1 may promote an inflammatory response.

Host cell apoptosis machinery is a frequent target of intracellular pathogens (Friedrich et al., 2017). Here we investigated the interaction of caspases in host cells with TLR4 signaling activated by lipopolysaccharide (LPS), a component of the gram-negative

Interdisciplinary Research Center on Biology and Chemistry, Shanghai Institute of Organic Chemistry, Chinese Academy of Sciences, PuDong District, Shanghai, China.

Correspondence to Junying Yuan: junying_yuan@sioc.ac.cn.

© 2021 Huang et al. This article is distributed under the terms of an Attribution–Noncommercial–Share Alike–No Mirror Sites license for the first six months after the publication date (see <http://www.rupress.org/terms/>). After six months it is available under a Creative Commons License (Attribution–Noncommercial–Share Alike 4.0 International license, as described at <https://creativecommons.org/licenses/by-nc-sa/4.0/>).

bacterial cell membrane, which promotes an innate immune response and is a contributor to various inflammatory pathologies in humans (Kawai and Akira, 2010). Activation of RIPK1 in macrophages stimulated by LPS in the presence of a pan-caspase inhibitor zVAD mimicking the inhibition of caspases such as caspase-8 has been shown to robustly induce the expression of a broad range of inflammatory molecules (Najjar et al., 2016). In this study, we used LPS/zVAD stimulation to model the condition where cells are infected by pathogens that can inhibit caspase activation. We investigated the signaling mechanism that induces the expression of proinflammatory cytokines downstream of TLR4 with caspase inhibition. Our study demonstrates that the proinflammatory cytokine production with LPS/zVAD stimulation is regulated by two-phase kinetics with an early RIPK1 scaffold-dependent but RIPK1 kinase-independent mechanism, which is followed by a prolonged inflammatory cytokine production that requires both RIPK1 scaffold and kinase functions. Furthermore, we show that autocrine production of TNF α connects the early mechanism with the late mechanism by promoting the activation of RIPK1 and the formation of a novel secondary signaling complex involving the scaffold function of RIPK1 and the key mediators of NF- κ B signaling to induce the expression of proinflammatory cytokines through an NF- κ B–RIPK1 kinase dual dependent pathway that is distinct from the canonical NF- κ B pathway and is negatively regulated by FADD and caspase-8.

Results

LPS/zVAD promotes inflammation with two distinct phases

To explore the mechanism of RIPK1 in regulating cytokine production, we stimulated BV2 cells, a mouse microglia-related cell line, with LPS alone or with LPS and pan-caspase inhibitor zVAD for different durations. We found that while treatment with LPS alone led to a transient increase in the transcription of proinflammatory cytokines and signaling mediators such as COX2 and NOS2, LPS/zVAD led to a prolonged increase in the transcription of proinflammatory factors that are inhibited by RIPK1 inhibitor Nec-1s (Fig. 1 A and Fig. S1 A). The effect of zVAD is at least in part mediated by blocking caspase-8-mediated cleavage of RIPK1, as blocking the cleavage of RIPK1 by D325H mutation also increased the transcription of IL6 when stimulated by LPS alone (Fig. S1 B), similar to that the peripheral blood mononuclear cells from patients with a point mutation inactivating the cleavage of human RIPK1 at D324 promote RIPK1-mediated inflammation (Tao et al., 2020). Consistently, in the culture medium of BV2 cells stimulated by LPS/zVAD for 4 h or longer, we detected a large amount of secreted IL6 and TNF α , which was reduced by the addition of RIPK1 kinase inhibitor Nec-1s (Fig. 1 B).

We further characterized the role of RIPK1 kinase on the temporal profile of the transcriptional response in BV2 cells treated with LPS/zVAD and observed a requirement of RIPK1 kinase for optimum induction of a variety of proinflammatory gene expression at the late phase. Induction of TNF α mRNA was robustly detected in BV2 cells treated with LPS/zVAD as early as 1 h; however, the addition of Nec-1s had little effect on this early

peak of TNF α or Cxcl2 transcription (Fig. 1 A and Fig. S1 A). Nec-1s only began to show an inhibitory effect on TNF α and Cxcl2 mRNA levels after stimulation with LPS/zVAD for 2–4 h or longer. Induction of IL6 transcription was detected with the treatment of LPS/zVAD for 4 h or longer, which was inhibited by Nec-1s (Fig. 1 A). The induction of NF- κ B target genes, such as Cox2 and Nos2, by LPS/zVAD showed similar profiles: The early induction was not affected by Nec-1s; Nec-1s only showed inhibition at 4 h or longer (Fig. S1 A). The production of proinflammatory cytokine IL6 was robustly induced by LPS alone in the early phase, but BV2 cells treated with LPS/zVAD produced elevated levels of IL6 for an extended period of time compared with that of LPS treatment alone (Fig. S1 C).

While treatment with LPS alone also led to increased production of IL6 and TNF α , the addition of Nec-1s had no effect on the production of IL6 and TNF α stimulated by LPS alone (Fig. S1 D). In agreement with the specific contribution of RIPK1 kinase to transcriptional responses upon LPS/zVAD induction, stimulation of BV2 cells with LPS/zVAD, but not with LPS alone, led to the activation of RIPK1, as indicated by p-S166 RIPK1, the biomarker of RIPK1 activation (Fig. 1 C; Degterev et al., 2008; Ofengeim et al., 2015). Stimulation of BV2 cells with zVAD alone for long periods (4–8 h) led to RIPK1 activation at low levels that were not sufficient to promote cytokine production (Fig. 1 C and Fig. S1 D). Thus, inhibition of caspase activity in cells stimulated by LPS promotes the activation of RIPK1 to mediate cytokine production after prolonged stimulation. RIPK1 knockout (KO) in BV2 cells also reduced the production of TNF α and IL6 in both early and late phases (Fig. 1 D), suggesting that the scaffold function of RIPK1 is involved in promoting proinflammatory cytokine production in both phases. Stimulation with LPS/zVAD or the addition of Nec-1s had no effect on the survival of BV2 cells (Fig. S1 E and F). Thus, LPS/zVAD can promote the activation of RIPK1 and production of proinflammatory cytokines without affecting cell survival.

We validated this finding in primary astrocytes, which do not express RIPK3, similar to BV2 cells (Fig. S2 A). Stimulating with LPS and zVAD together for 4 h or longer, but not with either agent alone, led to the activation of RIPK1 in primary astrocytes (Fig. 1 E and Fig. S2 B). The transcription and production of IL6 in primary astrocytes treated with both LPS and zVAD were prolonged compared with that of LPS alone (Fig. S2 C). Treatment with Nec-1s reduced the transcription and production of IL6 in primary astrocytes stimulated by LPS/zVAD but not by LPS alone (Fig. 1, F and G; and Fig. S2 D). Treatment of zVAD alone did not induce primary astrocytes to produce IL6 (Fig. S2 E). The viability of astrocytes was not affected by LPS or LPS/zVAD (Fig. S2 F). Consistently, mutant mouse primary astrocytes with genetic inactivation of RIPK1 kinase by knockin mutation D138N also showed reduced production of IL6 at later time points upon stimulation by LPS/zVAD (Fig. 1, H and I).

In addition, we also examined the response of primary *Ripk3*^{-/-} bone marrow-derived macrophages (BMDMs) to LPS/zVAD stimulation. We found that the transcriptional induction of IL6 in primary *Ripk3*^{-/-} BMDMs treated with LPS/zVAD for a long time was at a higher level than the treatment with LPS alone (Fig. S2 G). Treatment with Nec-1s inhibited the production of

experiments is shown (B). The cell lysates were immunoprecipitated (IP) with anti-p-S166 of RIPK1 antibody. The immunoprecipitates and cell lysates were analyzed by Western blotting (IB) with the indicated antibodies (C). (D) WT and *Ripk1*-KO BV2 cells were treated as indicated. The secretion levels of IL6 and TNF α were determined by ELISA. The mean of three technical repeats is shown ($n = 3$), and the results are representative of two independent experiments. NC, non-targeted control. (E) Primary astrocytes were treated as indicated. The cell lysates were analyzed by Western blotting with indicated antibodies. The graph is representative of three independent experiments. (F and G) Primary astrocytes were treated with LPS/zVAD with or without Nec-1s for the indicated periods of time. The cell culture medium was collected and analyzed by ELISA for secretion of IL6 (F). The transcription levels of *Il6* were analyzed by RT-qPCR assay (G). The mean of two independent experiments is shown ($n = 2$). (H) Primary WT and *Ripk1*^{D138N/D138N} astrocytes were treated with DMSO or LPS/zVAD for the indicated period of time. The cell culture medium was collected and analyzed by ELISA for secretion of IL6. The mean of three technical repeats is shown ($n = 3$), and the results are representative of two independent experiments. (I) WT and *Ripk1*^{D138N/D138N} primary astrocytes were treated as indicated for 8 h, and the cell lysates were collected for immunoblotting with the indicated antibodies. The graph is representative of three independent experiments. LPS 10 ng/ml (unless indicated); zVAD 50 μ M; Nec-1s 10 μ M. Error bars indicate SEM. *, nonspecific band.

IL6 and TNF α in *Ripk3*^{-/-} BMDMs treated LPS/zVAD but not with LPS alone (Fig. S2 H). Treatment with LPS/zVAD induced the activation of RIPK1, but not cell death, in *Ripk3*^{-/-} BMDMs (Fig. S2, I and J). Taken together, these results suggest that stimulation with LPS/zVAD can lead to RIPK1 kinase-independent production of inflammatory cytokines at early time points as well as RIPK1 kinase-dependent production of inflammatory cytokines at late time points in multiple cell types.

Polyinosinic:polycytidylic acid (poly(I:C))/zVAD also promotes sustained inflammation in an RIPK1-dependent manner

We next investigated if viral infection with caspase inhibition might also promote sustained inflammatory responses, as viral genomes often encode caspase inhibitors such as CrmA encoded by poxviruses that can inhibit both caspase-8 and caspase-1 (Bloomer et al., 2019; Stewart and Cookson, 2016). We used poly(I:C) to model viral infection. We found that treatment of BV2 cells with poly(I:C)/zVAD also led to sustained production of proinflammatory cytokines such as IL6, TNF, and Cxcl2 (Fig. S3 A). Poly(I:C)/zVAD stimulation of BV2 cells led to activation of RIPK1 (Fig. S3 B). The transcriptional induction of proinflammatory cytokines in BV2 cells stimulated by poly(I:C)/zVAD was inhibited by Nec-1s (Fig. S3 C). Stimulation of BV2 cells with poly(I:C)/zVAD had no effect on cell survival (Fig. S3 D).

Activation of RIPK1-dependent signaling in response to LPS/zVAD

We further dissected mechanisms underlying LPS/zVAD-mediated RIPK1 activation. MyD88 is an essential intracellular signaling mediator of TLR4 in cells stimulated by LPS (Takeda and Akira, 2004). We constructed *Myd88*-KO BV2 cells using CRISPR/Cas9. *Myd88* KO blocked both p-S166 RIPK1 and cytokine secretion stimulated by LPS/zVAD, including both early and late peaks (Fig. 2, A and B; and Fig. S4 A). TRIF (encoded by the TICAM1 gene) is a key mediator of TLR4 signaling and interacts with RIPK1 (Cusson-Hermance et al., 2005; Yamamoto et al., 2003). Consistently, knockdown of *Ticam1* also blocked the activation of RIPK1 and production of proinflammatory cytokines in BV2 cells stimulated by LPS/zVAD (Fig. S4, B and C).

To probe signaling events dependent upon the RIPK1 kinase downstream of TLR4, we characterized the profile of p-S166 RIPK1, p-S177/S176 IKK α / β , p-S32/S36 I κ B α , p-T180/Y182-p38, and p-T183/Y185-JNK in BV2 cells stimulated by LPS/zVAD (Fig. 2 C). We found that at early time points (0.5 and 2 h) when

p-S166 RIPK1 was not detectable, the addition of Nec-1s had no effect on the phosphorylation of IKK α / β , I κ B α , p38, or JNK. At later time points (4, 8, 12, and 24 h), however, the addition of Nec-1s inhibited the phosphorylation of IKK α / β , p38, or JNK and slightly reduced the phosphorylation of I κ B α . These results suggest that the activation of RIPK1 in BV2 cells with prolonged stimulation of LPS/zVAD regulates the activation of IKKs and MAPKs, including p38 and JNK.

We next considered the role of TNF α signaling, as TNFR1 is a well-established pathway to activate RIPK1 (Shan et al., 2018), and we generated *Tnf*-KO BV2 cells using CRISPR/Cas9 (Fig. S4 D). KO of *Tnf* blocked the appearance of p-S166 RIPK1 with LPS/zVAD stimulation (Fig. 2, D and E). These results suggest that TLR4 signal mediators MyD88 and TRIF as well as the autocrine production of TNF α are crucial for mediating RIPK1 activation and proinflammatory cytokine production in BV2 cells treated with LPS/zVAD.

KO of *Tnf* also reduced the phosphorylation of IKK α / β and JNK at the late time points (8 h and 12 h) but had little effect at the early time points (Fig. 2 D). The addition of exogenous TNF α to *Tnf*-KO BV2 cells with LPS/zVAD stimulation restored the appearance of p-S166 RIPK1, as well as the levels of p-IKK α / β and p-JNK, which were reduced upon the addition of Nec-1s (Fig. 2 E). KO of *Tnf* also blocked the transcription of *Il6* and *Il1 β* at late time points of LPS/zVAD treatment (Fig. 2 F). Taken together, these experiments suggest the important function of autocrine TNF α in promoting the activation of RIPK1 kinase and proinflammatory cytokine production in cells stimulated by LPS/zVAD.

Activated RIPK1 forms a signaling complex with TNFR1 in LPS/zVAD-treated cells

Since stimulation of TNFR1 by TNF α is known to promote the activation of RIPK1 (Shan et al., 2018), we next considered the possibility that autocrine production of TNF α may activate TNFR1 to promote the activation of RIPK1 in BV2 cells stimulated by LPS/zVAD. To test this possibility, we immunoprecipitated TNFR1 at different time points after the addition of LPS/zVAD, and, interestingly, we detected the presence of p-S166 RIPK1 in the TNFR1 immunocomplex at 8 and 12 h (Fig. 3 A). Thus, prolonged treatment with LPS/zVAD leads to the formation of a TNFR1/activated RIPK1 complex.

We next used mass spectrometry to explore the components of this signaling complex associated with activated RIPK1. An antibody for p-S166 RIPK1 (Ofengeim et al., 2015) was used to

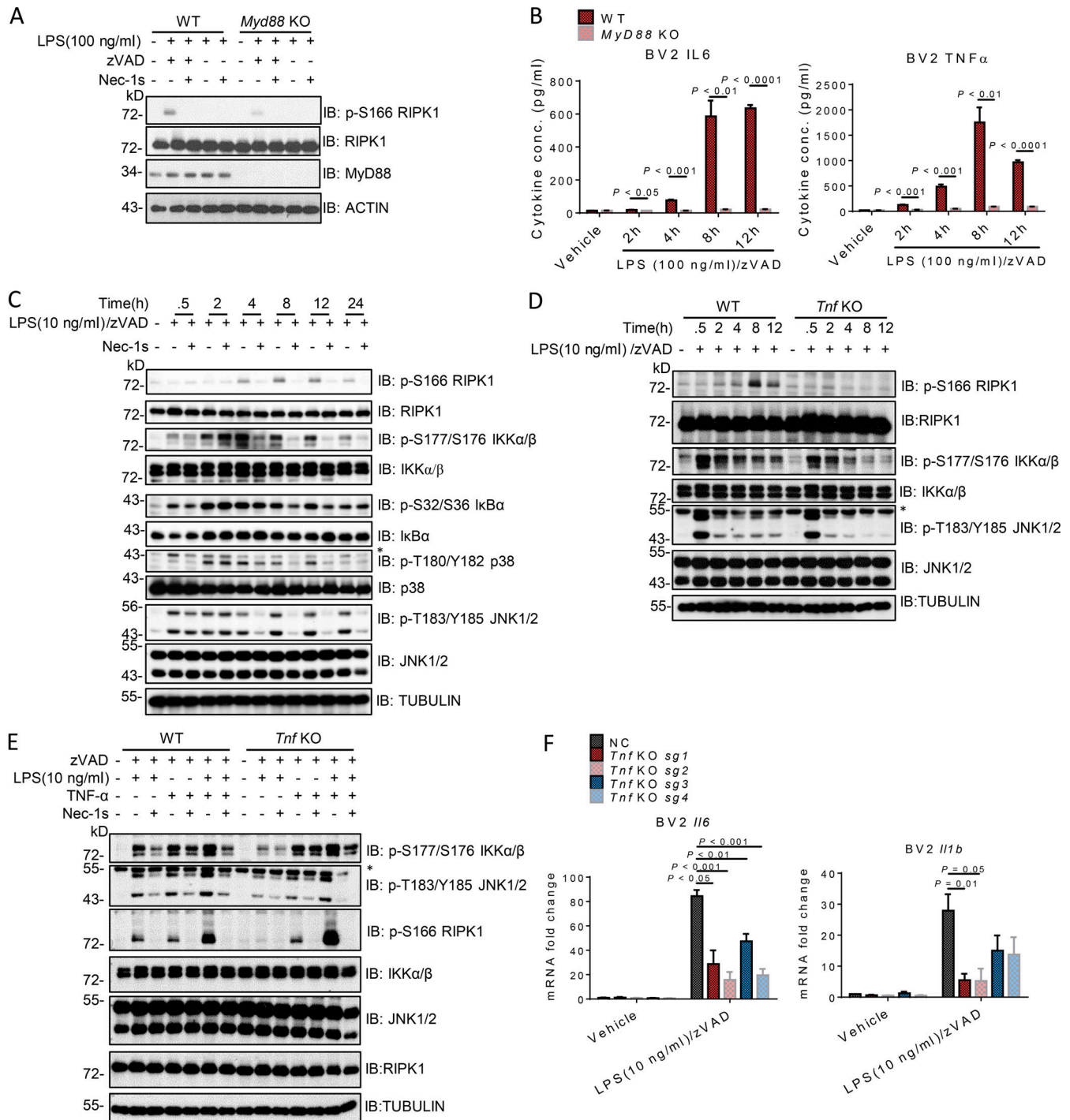


Figure 2. TLR mediates the activation of RIPK1 kinase in an Myd88 and TNF α pathway-dependent manner. (A) WT and MyD88-KO BV2 cells were treated as described for 8 h. The cell lysates were analyzed by Western blotting (IB) with the indicated antibodies. (B) WT and MyD88-KO BV2 cells were treated with DMSO or LPS/zVAD for the indicated periods of time. The cell culture medium was collected and analyzed by ELISA for secretion of TNF α and IL6, and the mean of three technical repeats is shown ($n = 3$). The results are representative of two independent experiments. (C and D) WT and Tnf-KO BV2 cells were treated as indicated, and cell lysates were analyzed by Western blotting with the indicated antibodies. (E) WT and Tnf-KO BV2 cells were treated as indicated for 8 h, and the cell lysates were analyzed by Western blotting with the antibodies indicated. (F) Control or Tnf-KO BV2 cells were treated as indicated for 8 h. The transcription levels of *Il1b* and *Il6* were analyzed by RT-qPCR assay, and the mean of two independent experiments is shown. LPS, 10 ng/ml or 100 ng/ml; zVAD, 50 μ M; TNF α , 100 ng/ml; Nec-1s, 10 μ M. Error bar represents SEM. Asterisks indicate nonspecific bands.

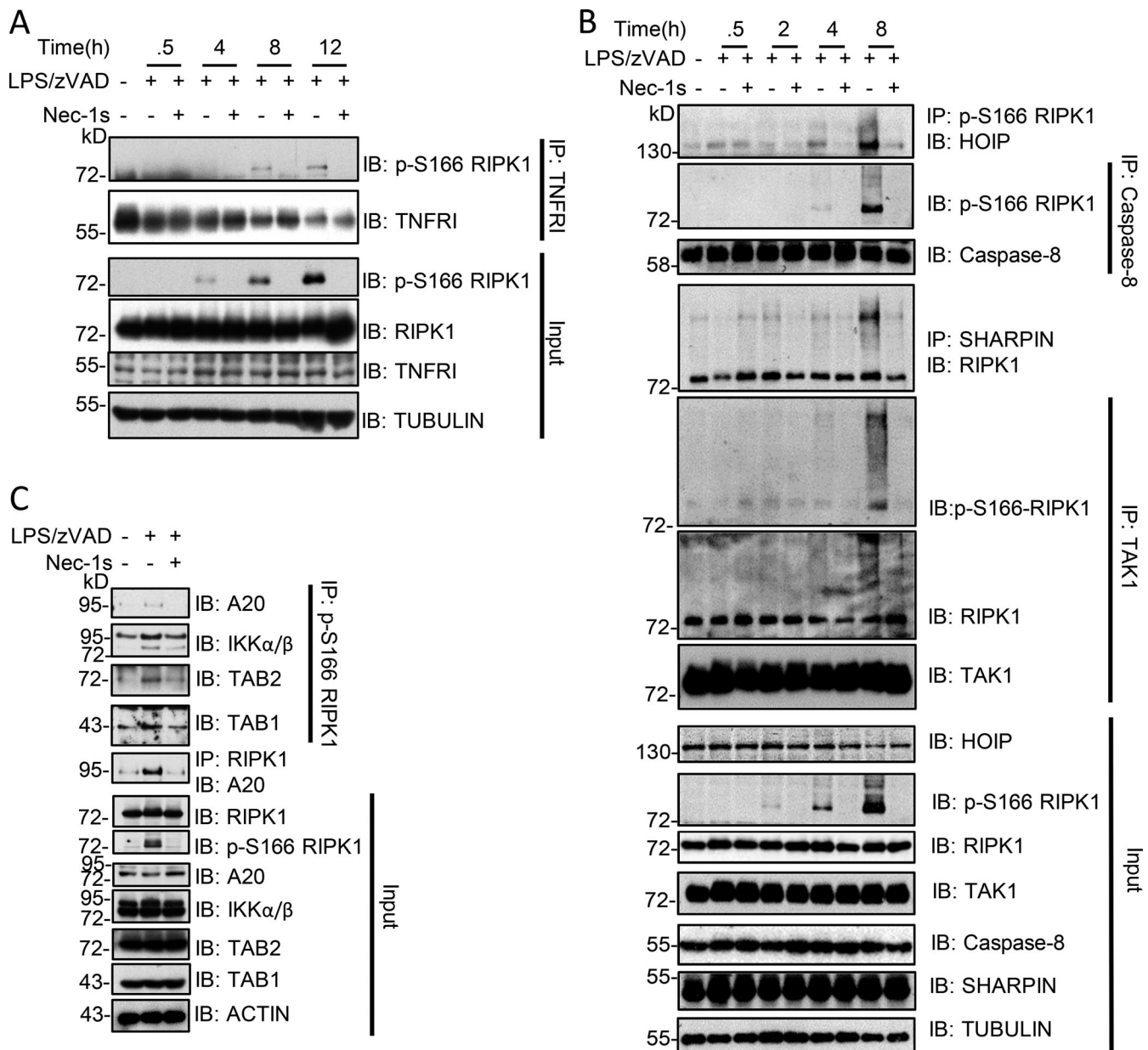


Figure 3. The formation of TNFR1-activated RIPK1 complex in cells treated with LPS/zVAD. (A and B) BV2 cells were treated as indicated. The cell lysates were immunoprecipitated (IP) with anti-TNFR1 antibody (A) or with anti-caspase-8 or anti-TAK1 antibody as indicated (B). The immunoprecipitates and cell lysates were analyzed by Western blotting (IB) with the indicated antibodies. **(C)** BV2 cells were treated as described for 8 h. The cell lysates were immunoprecipitated with anti-p-S166 RIPK1 or anti-RIPK1 antibody. The immunoprecipitates and cell lysates were analyzed by Western blotting with the indicated antibodies. LPS, 10 ng/ml; zVAD, 50 μ M; Nec-1s, 10 μ M.

isolate the complex associated with activated RIPK1 in BV2 cells stimulated with LPS/zVAD in the presence or absence of Nec-1s for 8 h. Interestingly, activated RIPK1 was found in association with multiple known components of TNFR1 complex I, such as TRADD, TRAF1/2 (TNFR-associated factor 1/2), TAK1 (TGF- β -activating kinase-1)/TAB1/2, A20, HOIP, and IKKs, as well as components of complex II, such as FADD, caspase-8 and cFLIP, which was inhibited by Nec-1s (Table S1). The presence of this signaling complex associated with activated RIPK1 in LPS/zVAD treated cells was further confirmed by immunoprecipitation. p-S166 RIPK1 was able to coimmunoprecipitate with caspase-8,

HOIP, SHARPIN, and TAK1 at the 8-h time point, but not earlier, with LPS/zVAD stimulation (Fig. 3 B). The binding of activated RIPK1 with caspase-8, HOIP, SHARPIN, TAK1, TAB1/2, IKK α / β , and A20 was blocked by Nec-1s (Fig. 3, B and C). Thus, LPS/zVAD stimulation leads to the interaction of RIPK1 with MyD88/IRAKs (IL-1 receptor-associated kinases) in the LPS signaling pathway independent of RIPK1 activity in the early phase, while the activation of RIPK1 promotes the formation of a signaling complex associated with TNFR1, which can lead to the production of proinflammatory cytokines in the late phase to mediate sustained inflammation.

Cytokine production induced by LPS/zVAD is regulated by FADD/Casp8 and NF- κ B

To elucidate the mechanism of RIPK1-mediated cytokine induction, we generated BV2 cells with KO of RelA (*Rela* KO), one of the central elements of the canonical NF- κ B pathway, using CRISPR/Cas9. In *Rela*-KO BV2 cells stimulated by prolonged LPS/zVAD treatment, the late transcription of CXCL2, IL1 β , and IL6 was reduced to variable degrees, and the addition of Nec-1s could still reduce their transcription at later time points (Fig. S4, E–G), suggesting the partial involvement of RelA/p65 in the late time points with LPS/zVAD stimulation.

Since FADD is critical for mediating the activation of caspase-8, which is inhibited by zVAD in our model, we next investigated the role of FADD in the cytokine production in BV2 cells stimulated by LPS. We found that FADD KO in BV2 cells had the opposite effect on the transcription of Il6 in the early versus late phase when stimulated by LPS alone (Fig. 4 A): KO FADD reduced the transcription of Il6 (<8 h), but it increased the transcription of Il6 with prolonged LPS stimulation (>16 h). Similarly, KO of caspase-8 reduced the transcription of Il6 (~1 h), but it highly stimulated the transcription of Il6 with prolonged LPS treatment (>16 h; Fig. 4 B).

We next investigated the role of FADD in this RIPK1-dependent signaling complex. FADD is a DD-containing adaptor protein that directly interacts with RIPK1-DD in complex II (Shan et al., 2018). Indeed, we detected robust interaction of activated RIPK1 with FADD in BV2 cells stimulated by LPS/zVAD, which was blocked by Nec-1s (Fig. 4 C). The binding of FADD and RIPK1 in BV2 cells stimulated by LPS/zVAD was TNF α dependent, as KO of TNF reduced the binding (Fig. 4 D). Interestingly, although FADD KO enhanced the activation of RIPK1(p-S166) in the absence or presence of stimulation, LPS/zVAD-stimulated phosphorylation of IKKs was reduced by FADD KO (Fig. 4 E). The transcription of Il6 in FADD-KO or caspase-8-KO BV2 cells induced by LPS was strongly inhibited by Nec-1s (Fig. 4, B and F). Caspase-8 KO stimulated the activation of RIPK1 but did not affect the binding of RIPK1 with FADD (Fig. S5 A). Taken together, these results suggest that activated RIPK1 recruits the key mediators of NF- κ B to promote an inflammatory response with prolonged LPS/zVAD treatment, while FADD or caspase-8 deficiency further enhances the activation of RIPK1 to promote the transcriptional induction of proinflammatory cytokines with prolonged LPS stimulation.

Discussion

In this study, we investigated the interaction of RIPK1 and caspases in the context of LPS stimulation. We found that caspase inhibition with either LPS or poly(I:C) stimulation leads to a biphasic kinetics of proinflammatory cytokine production: an early phase mediated by an RIPK1 scaffold-dependent but kinase-independent mechanism and a late phase mediated by a mechanism dependent upon both the scaffold and kinase functions of RIPK1. Prolonged treatment with LPS/zVAD promotes the formation of a complex including activated RIPK1 and the key components of the NF- κ B signaling complex, and thus, both kinase activity and scaffold functions of RIPK1 are involved in

mediating proinflammatory cytokine production in the late phase. With prolonged LPS stimulation and caspase inhibition, the activated RIPK1 serves to promote the scaffold function of RIPK1, which in turn recruits the key signaling mediators of the NF- κ B pathway to mediate the activation of inflammatory responses. Our study provides insights into the mechanism by which the kinase activity of RIPK1 may regulate its scaffold function. Since the canonical NF- κ B signaling is regulated independent of RIPK1 kinase, the formation of an RIPK1 kinase-dependent NF- κ B signaling complex with caspase inhibition provides an alternative mechanism, which we would like to term an “unconventional NF- κ B signaling” pathway, that may be involved in mediating RIPK1 kinase-dependent inflammatory processes under pathological conditions (Fig. S5 B). This unconventional NF- κ B signaling is positively regulated by RIPK1 kinase and negatively regulated by FADD and caspase-8. The complex that we have identified here includes activated RIPK1, IKKs, FADD, and caspase-8 functions differently from that of the “FADDosome” that mediates inflammatory response downstream of TRAIL (TNF-related apoptosis-inducing ligand) signaling, where FADD and caspase-8 were found to promote inflammation (Henry and Martin, 2017), which might be similar to the early phase with LPS/zVAD stimulation. Since mutant mice with conditional deletion of caspase-8 and FADD in intestinal epithelial cells develop colitis and ileitis that model human inflammatory bowel disease (Schwarzer et al., 2020), this unconventional NF- κ B signaling pathway involving activated RIPK1 and NF- κ B regulators may promote chronic inflammation in human inflammatory conditions.

MyD88 is a key signal mediator for all TLRs except TLR3 (Kawai and Akira, 2010). The binding and activation of IRAKs by MyD88 activate E3 ubiquitin ligase TRAF6 and TAK1, which in turn promote the activation of NF- κ B signaling. This canonical NF- κ B pathway mediates the transcription of proinflammatory genes and cytokines in cells stimulated by LPS alone and is likely responsible for the early induction of proinflammatory genes and cytokines in cells stimulated with LPS/zVAD as well. Prolonged stimulation of LPS/zVAD leads to a second wave of proinflammatory gene expression that is activated by autocrine production of TNF α and mediated by TNFR1, which forms a signaling complex including activated RIPK1, FADD, caspase-8, cFLIP, TRADD, TRAF1/2, TAK1, A20, HOIP, SHARPIN, and IKKs. Since this second wave of proinflammatory cytokine production can be enhanced by FADD and caspase-8 KO, our results reveal a mechanism by which FADD/caspase-8 suppress RIPK1 kinase in the TLR signaling pathway to negatively regulate the inflammatory response.

Our data provide further insights into the mechanism by which caspases negatively regulate the activation of RIPK1 in cells stimulated by TLR ligands in bacteria and viruses. TLR4-mediated activation of caspase-8 has been reported to occur in retinal ganglion cells in an acute glaucoma model (Chi et al., 2014). Activation of caspase-8 has also been found in microglia in response to LPS stimulation to regulate the inflammatory response without triggering cell death (Burguillos et al., 2011). Furthermore, the dysregulated activation of caspase-8 in neuroinflammation was also found in pathological conditions (e.g.,

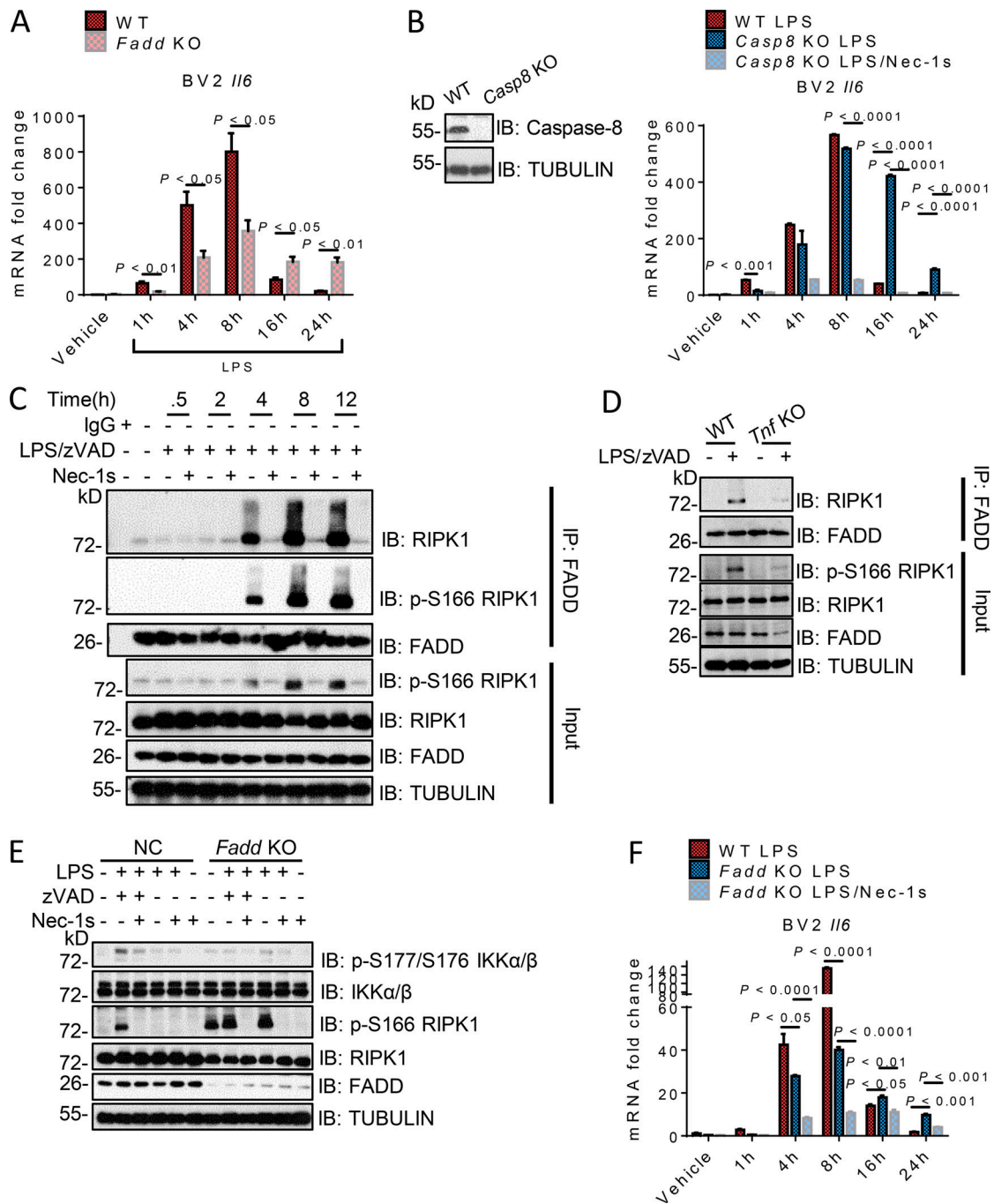


Figure 4. **RIPK1 kinase activity-regulated cytokine production is FADD/caspase-8 dependent.** (A) WT or *Fadd*-KO BV2 cells were treated as indicated. The transcription levels of *Il6* were analyzed by RT-qPCR assay, and the mean of three technical repeats ($n = 3$) is shown. The results are representative of two independent experiments. (B) WT and *Casp8*-KO BV2 cells were treated as indicated, and the transcription levels of *Il6* were measured by RT-qPCR assay. The mean of three technical repeats ($n = 3$) is shown. The results are representative of three independent experiments. (C) BV2 cells were treated as indicated. The cell lysates were immunoprecipitated (IP) with an anti-FADD antibody. The immunoprecipitates and cell lysates were analyzed by Western blotting (IB) with the indicated antibodies. (D) Control and *Tnf*-KO BV2 cells were treated as indicated for 8 h. The cell lysates were immunoprecipitated with anti-FADD antibody. The immunoprecipitates and cell lysates were analyzed by Western blotting with the indicated antibodies. (E) WT or *Fadd*-KO BV2 cells were treated as indicated for 8 h, and the cell lysates were analyzed by Western blotting with the indicated antibodies. NC, non-targeted control. (F) WT or *Fadd*-KO BV2 cells were treated as indicated. The transcription levels of *Il6* were analyzed by RT-qPCR assay. LPS, 10 ng/ml; zVAD, 50 μ M; Nec-1s, 10 μ M. Error bar indicates SEM.

in animal models of multiple sclerosis and postmortem pathological samples of patients with multiple sclerosis; Ofengeim et al., 2015). Since we found that this biphasic production of proinflammatory cytokines occurs without cell death, our results demonstrate a sustained proinflammatory cytokine production mechanism mediated by RIPK1 kinase activity that involves the NF- κ B pathway. Inflammation is often recognized as a double-edged sword, with early response implicated in the clearance of pathogens, while sustained inflammation often leads to pathology. Our results suggest that early and transient activation of inflammation mediated by the NF- κ B pathway independent of RIPK1 may primarily serve a beneficial function, while prolonged inflammatory conditions mediated by RIPK1 kinase may lead to deleterious consequences as in chronic inflammatory conditions.

Materials and methods

Reagents and antibodies

The following reagents were commercially purchased: LPS (Sigma-Aldrich; catalog no. L2630); zVAD.fmk (Selleckchem; catalog no. 187389-52-2), and recombinant mouse TNF α (Novoprotein; catalog no. CF09), R-7-Cl-O-Nec-1 (Nec-1s; custom synthesized) antibodies from Cell Signaling Technology against I κ B α (catalog no. 4814 from rabbit), p-I κ B α (Ser32; catalog no. 2859 from mouse), p65 (catalog no. 8242 from rabbit), p-p65 (Ser536; catalog no. 3033 from rabbit), IKK α (catalog no. 2682 from rabbit), IKK β (catalog no. 8943 from rabbit), RIPK1 (catalog no. 3493 from rabbit), caspase-8 (catalog no. 4927 from rabbit), TNFR1 (catalog no. 13377 from rabbit), p38 (catalog no. 9212 from rabbit), p-p38 (catalog no. 4511 from mouse), p-JNK1/2 (catalog no. 4668 from rabbit); and JNK1/2 (catalog no. 9252 from rabbit) and rabbit anti- α -tubulin (catalog no. PM054) from MBL. Rabbit anti-SHARPIN (catalog no. 18474-1-AP) was from ProteinTech. Rabbit anti-FADD (catalog no. 124812) was from Abcam, and rabbit TNFR1 antibody (catalog no. MAB430) was from R&D Systems. Goat FADD antibody (catalog no. sc-6036) and mouse caspase-8 antibody (catalog no. sc5263) for immunoprecipitation were from Santa Cruz Biotechnology. Rabbit anti-p-S166 RIPK1 (BX60008) and rabbit anti-RIPK1 (BX60005) were from MJS BioLynx. Mouse anti-HOIP antibody and mouse anti-A20 antibody were produced in-house. HRP-conjugated goat anti-rabbit IgG (H+L) secondary antibody (catalog no. 31460) and HRP-conjugated goat anti-mouse IgG (H+L) secondary antibody (catalog no. 31430) were from Thermo Fisher Scientific.

Animals

Ripk1^{D138N/D138N} mice were generated using the CRISPR/Cas9 system. Briefly, the mixture of single-guide RNA (sgRNA), donor DNA, and Cas9 mRNA was microinjected into the zygotes of C57BL/6 mice; sgRNA (5'-TGACAAAGGTGTGATACACA-3') targeted exon 4 of RIPK1 to direct Cas9 endonuclease to specifically cut the RIPK1 gene and induced a double-stranded break, then mutated the aspartate (GAC) to asparagine (AAC) at position 138 of RIPK1 through donor DNA-mediated homology-directed repair. *Ripk1*^{D138N/D138N} mice had been backcrossed to a C57BL/6 background over 10 generations. All animals were maintained in

a specific pathogen-free environment, and animal experiments were conducted according to the protocols approved by the Standing Animal Care Committee at the Interdisciplinary Research Center of Biology and Chemistry, Shanghai Institute of Organic Chemistry.

Cell culture and treatments

Mouse microglial cell line BV2, human embryonic kidney HEK293T cells (American Type Culture Collection; catalog no. CRL-3216), mouse fibroblast cell line L929 (American Type Culture Collection; catalog no. CCL-1), primary astrocytes, and primary BMDMs were cultured in DMEM (Gibco) supplemented with 10% FBS (Gibco) and 1% penicillin and streptomycin. Cells were cultured at 37°C in a humidified atmosphere with 5% CO₂. DMSO (<0.2%) was used as a vehicle-only control. Primary astrocytes were derived from cerebral cortices of neonatal mice. The cortices were lysed, and the resuspended cells were cultured for 14 d, followed by shaking for 8 h at 220 rpm to remove microglia and oligodendrocytes, and astrocytes were digested by trypsin and seeded to plates as needed for experiments. Primary BMDMs were isolated from bone marrow of posterior limbs of mice (14 wk of age). After selectively lysing RBCs, the remaining cells were induced to differentiate for 7 d in conditioned culture medium from L929 cells.

Cell viability assay

General cell survival was measured by the ATP luminescence assay CellTiter-Glo (Promega; catalog no. G7570). The percentage of viability was normalized to readouts of DMSO-treated cells. Cell death was determined by propidium iodide staining, and the percentage of propidium iodide-positive cells was normalized to a positive control treated with 0.1% Triton X-100 for 10 h. All experiments were conducted in 384-well plates with at least three biological replicates. Data were collected using a multimode plate reader (PerkinElmer).

Virus packaging and transduction

Recombinant lentivirus was packaged in HEK293T cells transfected with packaging plasmids. Specifically, one well of HEK293T cells in six-well plates was transfected with 2 μ g plasmids, including 1 μ g expression vector (LentiCRISPR version 2 vector, catalog no. 52961; Addgene) and the packaging plasmids (0.25 μ g pMD2.G, catalog no. 12259, and 0.75 μ g psPAX, catalog no. 12260; Addgene). 72 h later, the media containing the virus were collected and filtered through a 0.45- μ m polyvinylidene difluoride membrane (Millipore-Sigma). Transduction was performed by incubating cells with virus-containing media in the presence of 8 μ g/ml polybrene for 48 h. Cells were then selected with 5 μ g/ml and 10 μ g/ml puromycin successively (72 h for each concentration).

Quantitative PCR (qPCR) analysis

Total RNA was extracted and purified using RNAiso Plus Reagent (Takara). Total RNA from primary astrocytes and BMDMs was extracted using the RNeasy Mini Kit (Qiagen; catalog no. 74104). Reverse transcription reactions were performed with M-MLV reverse transcription (Takara; catalog no. 2640A). For

qPCR, SYBR Green Master Mix (Biotool; catalog no. 2120) was used in the QuantStudio 7 Real-Time PCR System (Applied Biosystems), and the PCR conditions were 50°C for 2 min and 95°C for 10 min and 40 cycles of 95°C for 15 s and 60°C for 1 min. Fold induction of gene expression was calculated using $\Delta\Delta Ct$ (cycle threshold) method. Namely, Ct values for genes of interest were normalized to Ct values of β -actin (mouse) and then to those of DMSO groups. The following primers were used: *Il6*, forward, 5'-GACAAAGCCAGAGTCCTTCA-3', reverse, 5'-TGGTCCTTGGCCACTCCTTC-3'; *Tnf*, forward, 5'-ATGAGAAGTTCCCAAATGGC-3', reverse, 5'-CTCCACTTGGTGGTTTGCTA-3'; *Cox2*, forward, 5'-CCCTGCTGCCGACACCTTC-3', reverse, 5'-CCAGCAACCCGGCCAGCAAT-3'; *Cxcl2*, forward, 5'-CTCTCAAGGGCGGTCAAAAAGTT-3', reverse, 5'-TCAGACAGCGAGGCACATCAGGTA-3'; *Nos2*, forward, 5'-GGAATTCACAGTCATCCGGTA-3', reverse, 5'-ACCAGAGGCAGCACATCAA-3'; *Il1b*, forward, 5'-TGAAGTTGACGGACCCAAA-3', reverse, 5'-AGCTTCTCCACAGCCACAAT-3'; *Actin*, forward, 5'-GAGATTACTGCCCTGGCTCCTA-3', reverse, 5'-TCATCGTACTCCTGCTTGCTGAT-3'.

Plasmid construction

The annealed sgRNA oligonucleotides were cloned into Lenti-CRISPR version 2 vector (Addgene; catalog no. 52961). All plasmids were confirmed by sequencing. The following sgRNAs were used: sgRIPK1_Sense (S): 5'-CACCGACCTAGACAGCGGAGGCTTC-3', sgRIPK1_Antisense (AS): 5'-AAACGAAGCCTCCGCTGTCTAGGTC-3'; sgFADD #1_S: 5'-CACCGTTGCTTTGCTCAGCGCTCG-3', sgFADD#1_AS: 5'-AAACCGAGCGGTGAGCAAACGAAAC-3'; sgFADD #2_S: 5'-CACCGCGCGGTGAGCAAACGAAAGC-3', sgFADD #2_AS: 5'-AAACGCTTTGCTTTGCTCAGCGCC-3'; sgTNF α #1_S: 5'-CACCGAGAAAGCATGATCCGCGACG-3', sgTNF α #1_AS: 5'-AAACCGTCCGGATCATGCTTTCTC-3'; sgTNF α #2_S: 5'-CACCGTCCGGGTGATCGGTCCCAA-3', sgTNF α #2_AS: 5'-AAACTTGGGACCGATCACCCGAC-3'; sgTNF α #3_S: 5'-CACCGCATGATCGCGACGTGGAAC-3', sgTNF α #3_AS: 5'-AAACGTTCCACGTCGCGGATCATGC-3'; sgTNF α #4_S: 5'-CACCGCGGGGTGATCGGTCCC AAA-3', sgTNF α #4_AS: 5'-AAACTTTGGGACCGATCACCCGCGC-3'; sgRela_S: 5'-CACCGATCGAACAGCCGAAGCAACG-3', sgRela_AS: 5'-AAACCGTTGCTTCGGCTGTTTCGATC-3'; sgMyD88_S: 5'-CACCGCCCTTGGTCCGCTTAACGT-3', sgMyD88_AS: 5'-AAACAGTTAAGCGGACCAAGGGC-3'; sgCasp8_S: 5'-CACCGAGTCTAGGAAGT TGACCAGC-3', sgCasp8_AS: 5'-AAACGCTGGTCAACTTCTAGACTC-3'.

RNAi

BV2 cells were transfected with 25 nM siRNA using Lipofectamine RNAiMAX (Invitrogen) following the manufacturer's instruction. The sense sequence of mouse *Ticam1* siRNA is 5'-CTGGCTGAGGAGAACCTGTG-3'. The sequence for knockdown efficiency confirmation is forward, 5'-CTGGCTGAGGAGAACCTGTG-3', reverse, 5'-TGGCTGATCTCTAGGTGGCT-3'.

Immunoprecipitation

After cells were treated as described, media were removed, plates were placed on ice, and cells were washed with ice-cold PBS. Cells were then lysed in precooling NP-40 lysis buffer (20 mM Tris-HCl, pH 7.5, 150 mM NaCl, 1 mM EDTA, 1 mM

EGTA, 1% NP-40, 5 mM NaF, 1 mM β -glycerophosphate) supplemented with protease inhibitor cocktail (Biotool), sodium orthovanadate, and PMSF. Cell lysates were incubated on ice for 10 min and clarified at 15,000 $\times g$ for 15 min at 4°C. Lysates were then incubated with corresponding antibodies overnight, followed by incubation with protein G agarose (Thermo Fisher Scientific) for 4 h at 4°C. After four washes with cold NP-40 lysis buffer, the beads were boiled in SDS loading buffer (50 mM Tris-HCl, pH 6.8, 2% SDS, 10% glycerol, and 50 mM DTT) for 10 min.

Western blotting

Cell extracts or immunoprecipitates in SDS loading buffer were analyzed by SDS-PAGE. After transfer of resolved proteins to nitrocellulose membrane (EMD Millipore), the membranes were blocked with 5% BSA in 0.1% Tween with TBS for 30 min at room temperature and then successively incubated with primary antibodies overnight at 4°C and the peroxidase-coupled secondary antibody for 2 h at room temperature. Proteins were visualized by ECL. All immunoblots from cell samples were repeated at least two or three times independently with similar results.

Sample preparation for mass spectrometry

BV2 cells were treated with DMSO or 10 ng/ml LPS and 50 μ M zVAD with or without 10 μ M Nec-1s for 8 h. Cell lysates were collected and successively incubated with the indicated antibody and protein G agarose for immunoprecipitation. The protein G agarose/protein complexes were washed with NP-40 lysis buffer five times and double-distilled water five times.

Mass spectrometry

The binding proteins of activated RIPK1 were immunoprecipitated using anti-pS166 RIPK1 antibody and were trypsin digested on beads. The desalted peptides were analyzed on a Q Exactive HF-X Hybrid Quadrupole-Orbitrap mass spectrometer (Thermo Fisher Scientific). Protein identification was performed using Proteome Discoverer 2.2. The tandem mass spectra were searched against the UniProt mouse protein database. The precursor tolerance was set as 10 parts per million, and the fragment mass tolerance was set as 0.02 D. The cysteine carbamidomethylation was set as a static modification, and the methionine oxidation and protein N-terminal acetylation were set as variable modifications. The false discovery rates at peptide spectrum match level and protein level were controlled below 1%.

ELISA

Culture supernatants were collected, and commercial ELISA kits (R&D Systems) were used according to the manufacturer's instructions for measuring TNF α (catalog no. DY410) and IL6 (catalog no. DY406) secretion.

Statistics

Statistical analysis was performed using GraphPad Prism 5 software (GraphPad Software, Inc.). In all tests, a 95% confidence interval was used, for which $P < 0.05$ was considered a significant difference. The statistical comparisons were performed

using an unpaired two-tailed Student's *t* test between two groups, or one-way ANOVA with Dunnett's multiple comparison test among multiple groups with a single control, or two-way ANOVA with Bonferroni's multiple comparison test among different groups. Each experiment was repeated at least two or three times.

Online supplemental material

Fig. S1 demonstrates that RIPK1 kinase activity regulates cytokine production with LPS/zVAD stimulation in the absence of cell death in BV2 cells. **Fig. S2** shows that RIPK1 kinase activity regulates cytokine production with LPS/zVAD stimulation in primary astrocytes and BMDMs. **Fig. S3** displays the RIPK1 kinase-dependent inflammation induced by other TLR pathways. **Fig. S4** portrays the effect of Myd88, TRIF, and NF- κ B pathways in LPS/zVAD-induced inflammation. **Fig. S5** illustrates the effect of caspase-8 in RIPK1-FADD interaction and summarizes the mechanism scheme of RIPK1 kinase-dependent inflammation. Table S1 lists peptides of the proteins interacting with activated RIPK1 identified by mass spectrometry.

Acknowledgments

This work was supported in part by the National Key R&D Program of China (2016YFA0501900), the National Natural Science Foundation of China (31530041, 21837004, and 91849204), the Chinese Academy of Sciences (XDB39030000), and the Shanghai Municipal Science and Technology Major Project (2019SHZDZX02).

J. Yuan is a consultant for Denali Therapeutics and Sanofi, which are developing RIPK1 inhibitors. The other authors declare no competing financial interests.

Author contributions: This project was designed and directed by J. Yuan. X. Huang conducted most of the experiments. S. Tan, Y. Li, and X. Li assisted with some data collection. S. Cao and B. Shan conducted mass spectrometric analysis. H. Pan and L. Qian assisted with advising X. Huang. The manuscript was written by J. Yuan and X. Huang.

Submitted: 21 July 2020

Revised: 8 January 2021

Accepted: 22 February 2021

References

Bloomer, D.T., T. Kitevska-Ilioski, D. Pantaki-Eimany, Y. Ji, M.A. Miles, B. Heras, and C.J. Hawkins. 2019. CrmA orthologs from diverse poxviruses potentially inhibit caspases-1 and -8, yet cleavage site mutagenesis frequently produces caspase-1-specific variants. *Biochem. J.* 476:1335–1357. <https://doi.org/10.1042/BCJ20190202>

Burguillos, M.A., T. Deierborg, E. Kavanagh, A. Persson, N. Hajji, A. Garcia-Quintanilla, J. Cano, P. Brundin, E. Englund, J.L. Venero, et al. 2011. Caspase signalling controls microglia activation and neurotoxicity. *Nature*. 472:319–324. <https://doi.org/10.1038/nature09788>

Chi, W., F. Li, H. Chen, Y. Wang, Y. Zhu, X. Yang, J. Zhu, F. Wu, H. Ouyang, J. Ge, et al. 2014. Caspase-8 promotes NLRP1/NLRP3 inflammasome activation and IL-1 β production in acute glaucoma. *Proc. Natl. Acad. Sci. USA*. 111:11181–11186. <https://doi.org/10.1073/pnas.1402819111>

Cusson-Hermance, N., S. Khurana, T.H. Lee, K.A. Fitzgerald, and M.A. Keller. 2005. Rip1 mediates the Trif-dependent Toll-like receptor 3- and

4-induced NF- κ B activation but does not contribute to interferon regulatory factor 3 activation. *J. Biol. Chem.* 280:36560–36566. <https://doi.org/10.1074/jbc.M506831200>

Degterev, A., J. Hitomi, M. Germesheid, I.L. Ch'en, O. Korkina, X. Teng, D. Abbott, G.D. Cuny, C. Yuan, G. Wagner, et al. 2008. Identification of RIP1 kinase as a specific cellular target of necrostatins. *Nat. Chem. Biol.* 4:313–321. <https://doi.org/10.1038/nchembio.83>

Friedrich, A., J. Pechstein, C. Berens, and A. Lührmann. 2017. Modulation of host cell apoptotic pathways by intracellular pathogens. *Curr. Opin. Microbiol.* 35:88–99. <https://doi.org/10.1016/j.mib.2017.03.001>

Henry, C.M., and S.J. Martin. 2017. Caspase-8 acts in a non-enzymatic role as a scaffold for assembly of a pro-inflammatory "FADDosome" complex upon TRAIL stimulation. *Mol. Cell.* 65:715–729.e5. <https://doi.org/10.1016/j.molcel.2017.01.022>

Kawai, T., and S. Akira. 2010. The role of pattern-recognition receptors in innate immunity: update on Toll-like receptors. *Nat. Immunol.* 11:373–384. <https://doi.org/10.1038/ni.1863>

Lalaoui, N., S.E. Boyden, H. Oda, G.M. Wood, D.L. Stone, D. Chau, L. Liu, M. Stoffels, T. Kratina, K.E. Lawlor, et al. 2020. Mutations that prevent caspase cleavage of RIPK1 cause autoinflammatory disease. *Nature*. 577:103–108. <https://doi.org/10.1038/s41586-019-1828-5>

Lin, Y., A. Devin, Y. Rodriguez, and Z.G. Liu. 1999. Cleavage of the death domain kinase RIP by caspase-8 prompts TNF-induced apoptosis. *Genes Dev.* 13:2514–2526. <https://doi.org/10.1101/gad.13.19.2514>

Meng, H., Z. Liu, X. Li, H. Wang, T. Jin, G. Wu, B. Shan, D.E. Christofferson, C. Qi, Q. Yu, et al. 2018. Death-domain dimerization-mediated activation of RIPK1 controls necroptosis and RIPK1-dependent apoptosis. *Proc. Natl. Acad. Sci. USA*. 115:E2001–E2009. <https://doi.org/10.1073/pnas.1722013115>

Mifflin, L., D. Ofengeim, and J. Yuan. 2020. Receptor-interacting protein kinase 1 (RIPK1) as a therapeutic target. *Nat. Rev. Drug Discov.* 19:553–571. <https://doi.org/10.1038/s41573-020-0071-y>

Najjar, M., D. Saleh, M. Zelic, S. Nogusa, S. Shah, A. Tai, J.N. Finger, A. Polykratis, P.J. Gough, J. Bertin, et al. 2016. RIPK1 and RIPK3 kinases promote cell-death-independent inflammation by Toll-like receptor 4. *Immunity*. 45:46–59. <https://doi.org/10.1016/j.immuni.2016.06.007>

Newton, K., K.E. Wickliffe, D.L. Dugger, A. Maltzman, M. Roose-Girma, M. Dohse, L. Kómúves, J.D. Webster, and V.M. Dixit. 2019. Cleavage of RIPK1 by caspase-8 is crucial for limiting apoptosis and necroptosis. *Nature*. 574:428–431. <https://doi.org/10.1038/s41586-019-1548-x>

Ofengeim, D., and J. Yuan. 2013. Regulation of RIP1 kinase signalling at the crossroads of inflammation and cell death. *Nat. Rev. Mol. Cell Biol.* 14:727–736. <https://doi.org/10.1038/nrm3683>

Ofengeim, D., Y. Ito, A. Najafav, Y. Zhang, B. Shan, J.P. DeWitt, J. Ye, X. Zhang, A. Chang, H. Vakifahmetoglu-Norberg, et al. 2015. Activation of necroptosis in multiple sclerosis. *Cell Rep.* 10:1836–1849. <https://doi.org/10.1016/j.celrep.2015.02.051>

Schwarzer, R., H. Jiao, L. Wachsmuth, A. Tresch, and M. Pasparakis. 2020. FADD and caspase-8 regulate gut homeostasis and inflammation by controlling MLKL- and GSDMD-mediated death of intestinal epithelial cells. *Immunity*. 52:978–993.e6. <https://doi.org/10.1016/j.immuni.2020.04.002>

Shan, B., H. Pan, A. Najafav, and J. Yuan. 2018. Necroptosis in development and diseases. *Genes Dev.* 32:327–340. <https://doi.org/10.1101/gad.312561.118>

Stewart, M.K., and B.T. Cookson. 2016. Evasion and interference: intracellular pathogens modulate caspase-dependent inflammatory responses. *Nat. Rev. Microbiol.* 14:346–359. <https://doi.org/10.1038/nrmicro.2016.50>

Takeda, K., and S. Akira. 2004. TLR signaling pathways. *Semin. Immunol.* 16:3–9. <https://doi.org/10.1016/j.smim.2003.10.003>

Tao, P., J. Sun, Z. Wu, S. Wang, J. Wang, W. Li, H. Pan, R. Bai, J. Zhang, Y. Wang, et al. 2020. A dominant autoinflammatory disease caused by non-cleavable variants of RIPK1. *Nature*. 577:109–114. <https://doi.org/10.1038/s41586-019-1830-y>

Wallach, D., T.B. Kang, C.P. Dillon, and D.R. Green. 2016. Programmed necrosis in inflammation: toward identification of the effector molecules. *Science*. 352:aaf2154. <https://doi.org/10.1126/science.aaf2154>

Xu, D., T. Jin, H. Zhu, H. Chen, D. Ofengeim, C. Zou, L. Mifflin, L. Pan, P. Amin, W. Li, et al. 2018. TBK1 suppresses RIPK1-driven apoptosis and inflammation during development and in aging. *Cell*. 174:1477–1491.e19. <https://doi.org/10.1016/j.cell.2018.07.041>

- Yamamoto, M., S. Sato, H. Hemmi, K. Hoshino, T. Kaisho, H. Sanjo, O. Takeuchi, M. Sugiyama, M. Okabe, K. Takeda, et al. 2003. Role of adaptor TRIF in the MyD88-independent Toll-like receptor signaling pathway. *Science*. 301:640–643. <https://doi.org/10.1126/science.1087262>
- Yuan, J., A. Najafzadeh, and B.F. Py. 2016. Roles of caspases in necrotic cell death. *Cell*. 167:1693–1704. <https://doi.org/10.1016/j.cell.2016.11.047>
- Yuan, J., P. Amin, and D. Ofengeim. 2019. Necroptosis and RIPK1-mediated neuroinflammation in CNS diseases. *Nat. Rev. Neurosci.* 20:19–33. <https://doi.org/10.1038/s41583-018-0093-1>
- Zhang, X., J.P. Dowling, and J. Zhang. 2019. RIPK1 can mediate apoptosis in addition to necroptosis during embryonic development. *Cell Death Dis.* 10:245. <https://doi.org/10.1038/s41419-019-1490-8>

Supplemental material

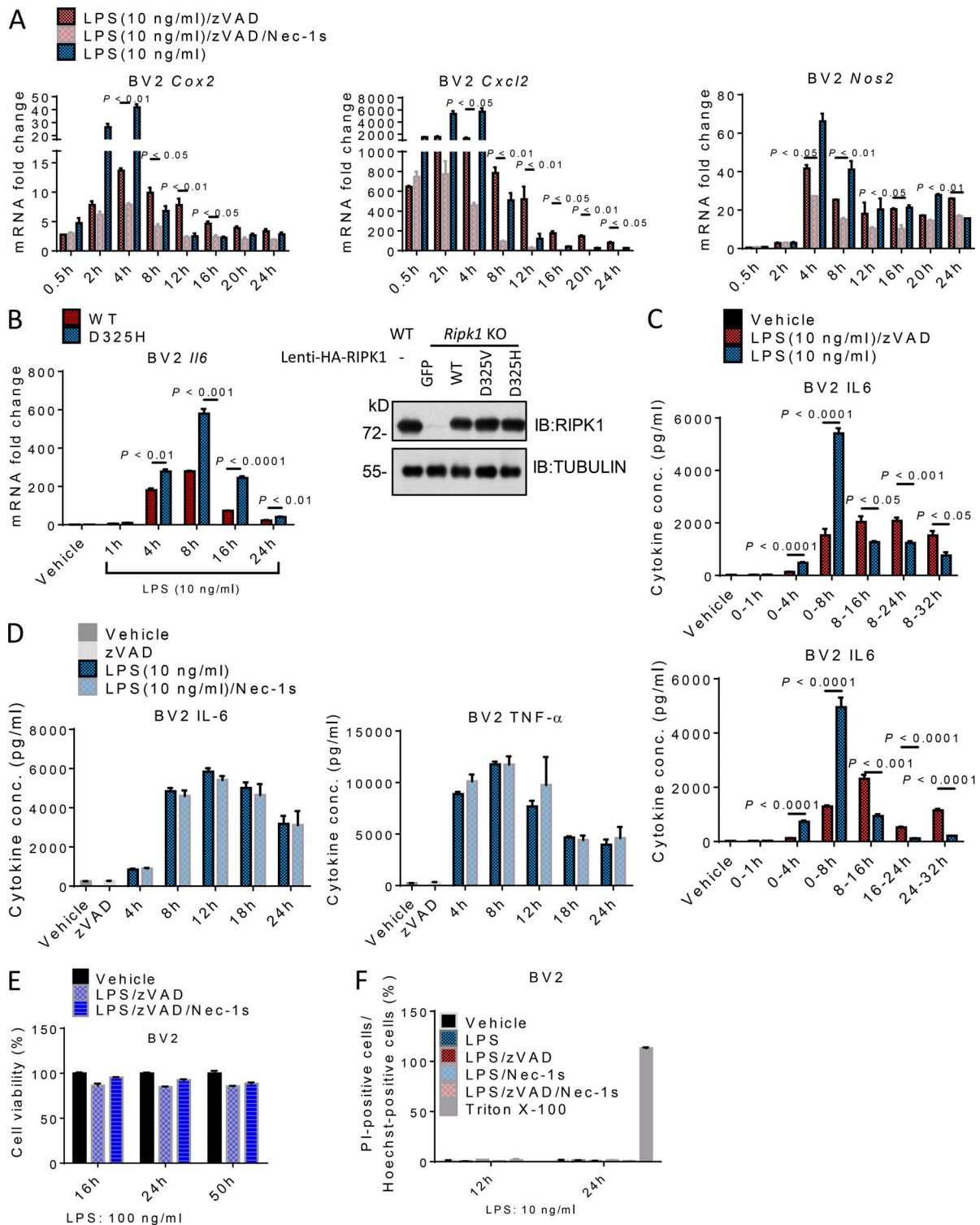


Figure S1. **RIPK1 kinase activity regulates cytokine production with LPS/zVAD stimulation.** (A) BV2 cells were treated for different time periods as indicated. The transcription levels of *Cox2*, *Cxcl2*, and *Nos2* were analyzed by RT-qPCR assay. The mean of two or four technical repeats ($n = 2$ or 4) is shown. The results are representative of two independent experiments. (B) RIPK1-KO BV2 cells were reconstituted with WT RIPK1 or D325H RIPK1 mutant and treated as indicated. Cell lysates were analyzed by Western blotting (IB) with the indicated antibodies, and the transcription levels of *Il6* were determined by RT-qPCR assay. The mean of three technical repeats ($n = 3$) is shown, and the results are representative of three independent experiments. (C) The culture medium from BV2 cells treated with LPS or LPS/zVAD for the indicated periods of time was assayed for IL6 levels using an ELISA kit, and the mean of two independent experiments ($n = 2$) is shown. (D) BV2 cells were treated as indicated. zVAD treatment was for 24 h. The cell culture medium was collected and analyzed by ELISA for secretion of TNF α and IL6, and the mean of three independent experiments is shown ($n = 3$). (E and F) BV2 cells were treated as indicated; cell viability was determined by CellTiter-Glo assay (E); and cell death was determined by propidium iodide (PI) staining (F). The mean of three independent experiments is shown ($n = 3$). LPS, 10 ng/ml or 100 ng/ml as indicated; zVAD, 50 μ M; Nec-1s, 10 μ M. Error bar represents SEM.

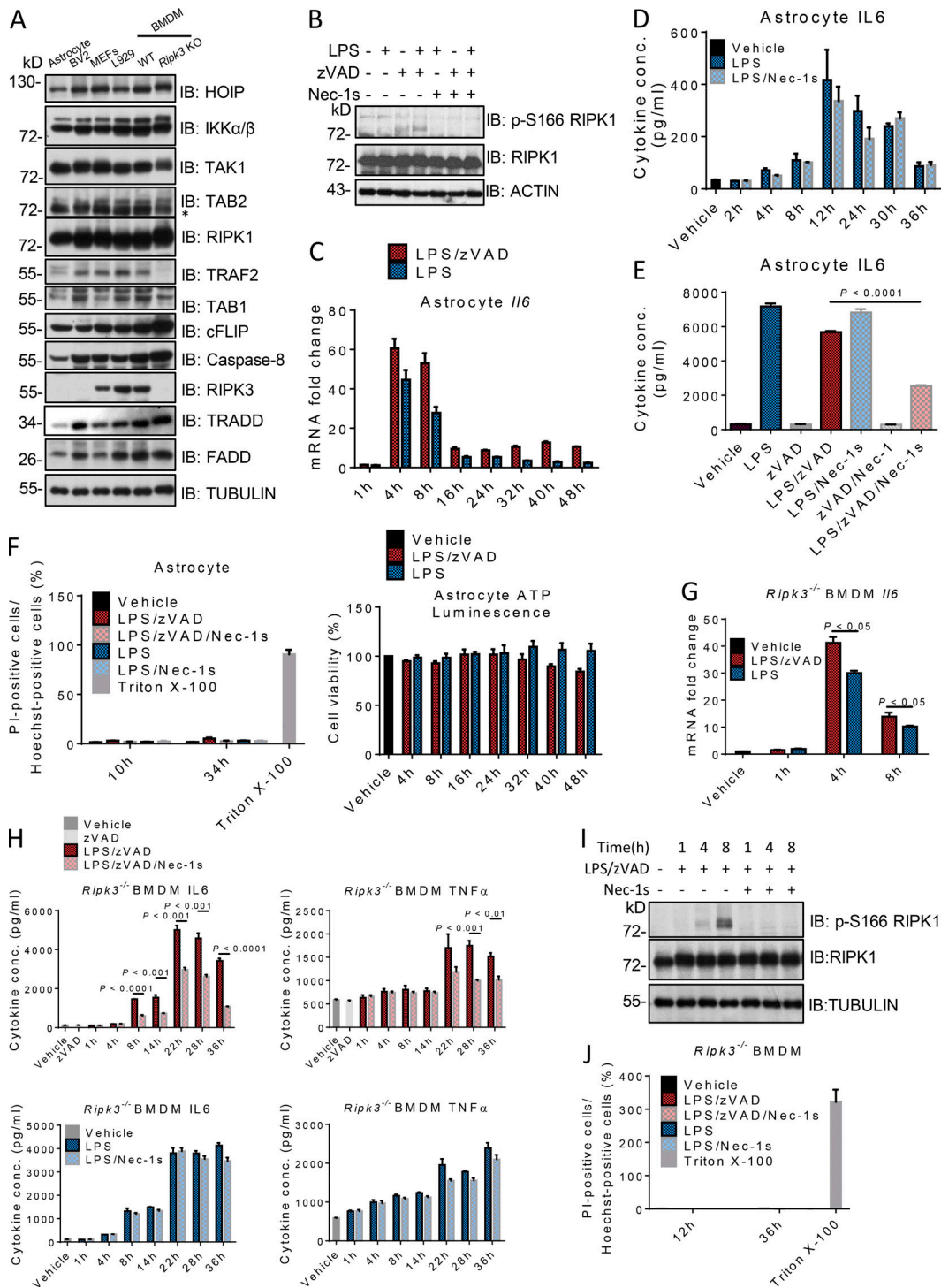


Figure S2. RIPK1 kinase activity regulates cytokine production with LPS/zVAD stimulation in primary astrocytes and BMDMs. (A) Cell lysates from the indicated types of cells were analyzed by Western blotting (IB) with the indicated antibodies. (B) Primary astrocytes were treated as indicated, and the cell lysates were collected for Western blotting with the indicated antibodies. (C and D) Primary mouse astrocytes were treated as indicated. The transcription and secretion levels of IL6 were measured by RT-qPCR assay (C) and ELISA (D), respectively. The mean of three technical repeats (C; $n = 3$) or the mean of two independent experiments (D; $n = 2$) is shown. (E) Primary astrocytes were treated as indicated for 8 h. The cell culture medium was collected and analyzed by ELISA for secretion of IL6. The mean of three technical repeats ($n = 3$) is shown, and the results are representative of two independent experiments. (F) Cell viability of primary astrocytes treated as indicated was determined by propidium iodide (PI) staining and CellTiter-Glo assay. The mean of three independent experiments is shown ($n = 3$). (G and H) Primary *Ripp3*^{-/-} BMDMs were treated as indicated, and cytokine transcription levels were measured by RT-qPCR assay. IL6 and TNF α secreted in the medium were analyzed by ELISA. The mean of three technical repeats (G; $n = 3$) or the mean of two independent experiments (H; $n = 2$) is shown. (I) Primary *Ripp3*^{-/-} BMDMs were treated as indicated, and the cell lysates were analyzed by Western blotting with the indicated antibodies. (J) Cell viability of primary *Ripp3*^{-/-} BMDMs treated as indicated was determined by PI staining. The mean of three independent experiments ($n = 3$) is shown. LPS, 10 ng/ml; zVAD, 50 μ M; Nec-1s, 10 μ M. Error bar indicates SEM. The asterisk in A indicates a nonspecific band.

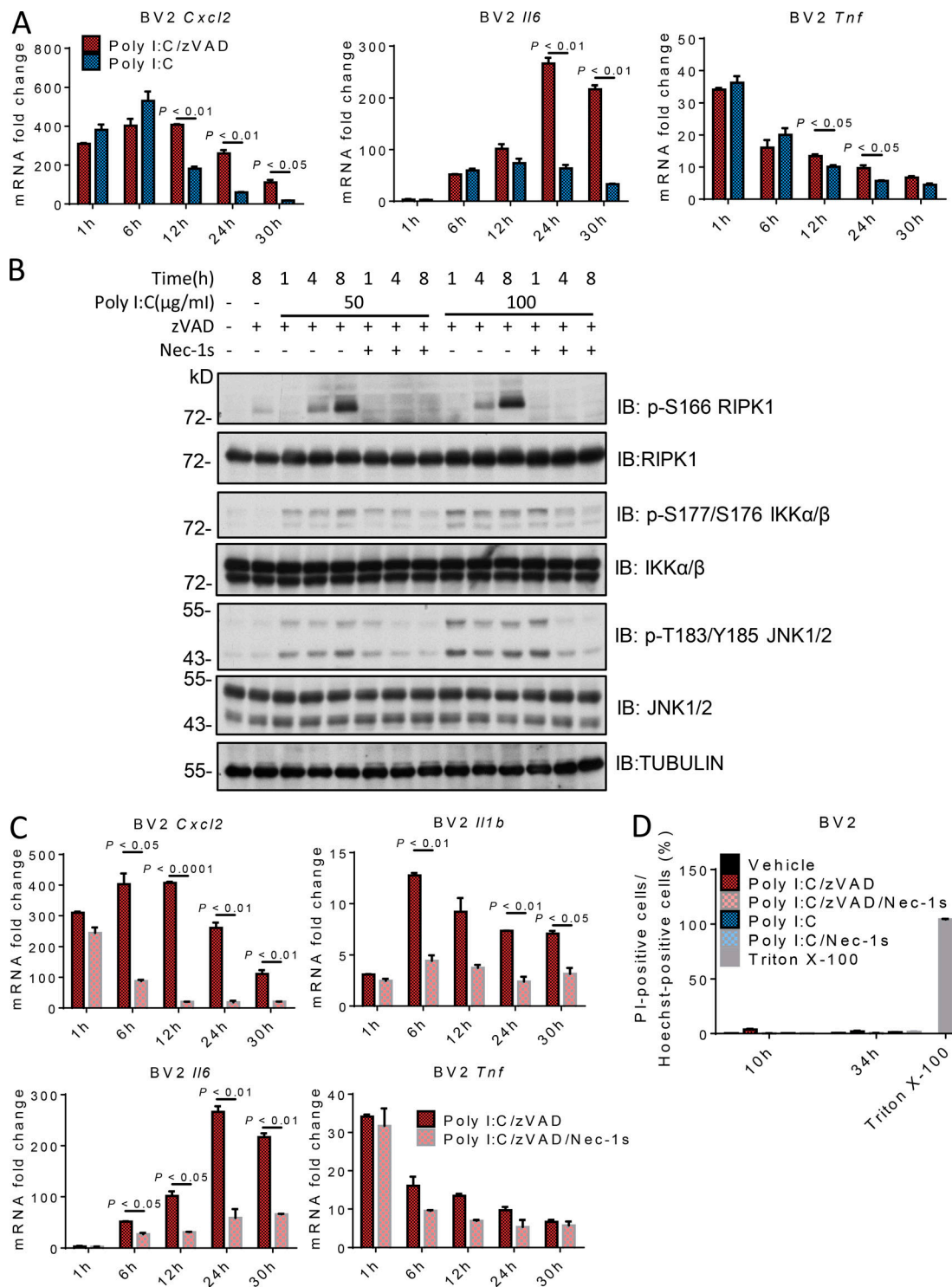


Figure S3. **RIPK1 kinase-dependent inflammation induced by other TLR pathways.** (A and C) BV2 cells were treated as indicated, and cytokine transcription levels were measured by RT-qPCR assay. The mean of three technical repeats is shown ($n = 3$), and the results are representative of two independent experiments. (B) BV2 cells were treated as indicated, and the cell lysates were analyzed by Western blotting (IB) with the indicated antibodies. (D) The viability of BV2 cells treated as indicated was determined by propidium iodide (PI) staining, and the mean of three independent experiments is shown ($n = 3$). Poly(I:C), 100 μg/ml (unless indicated); zVAD, 50 μM; Nec-1s, 10 μM. Data are shown as mean ± SEM.

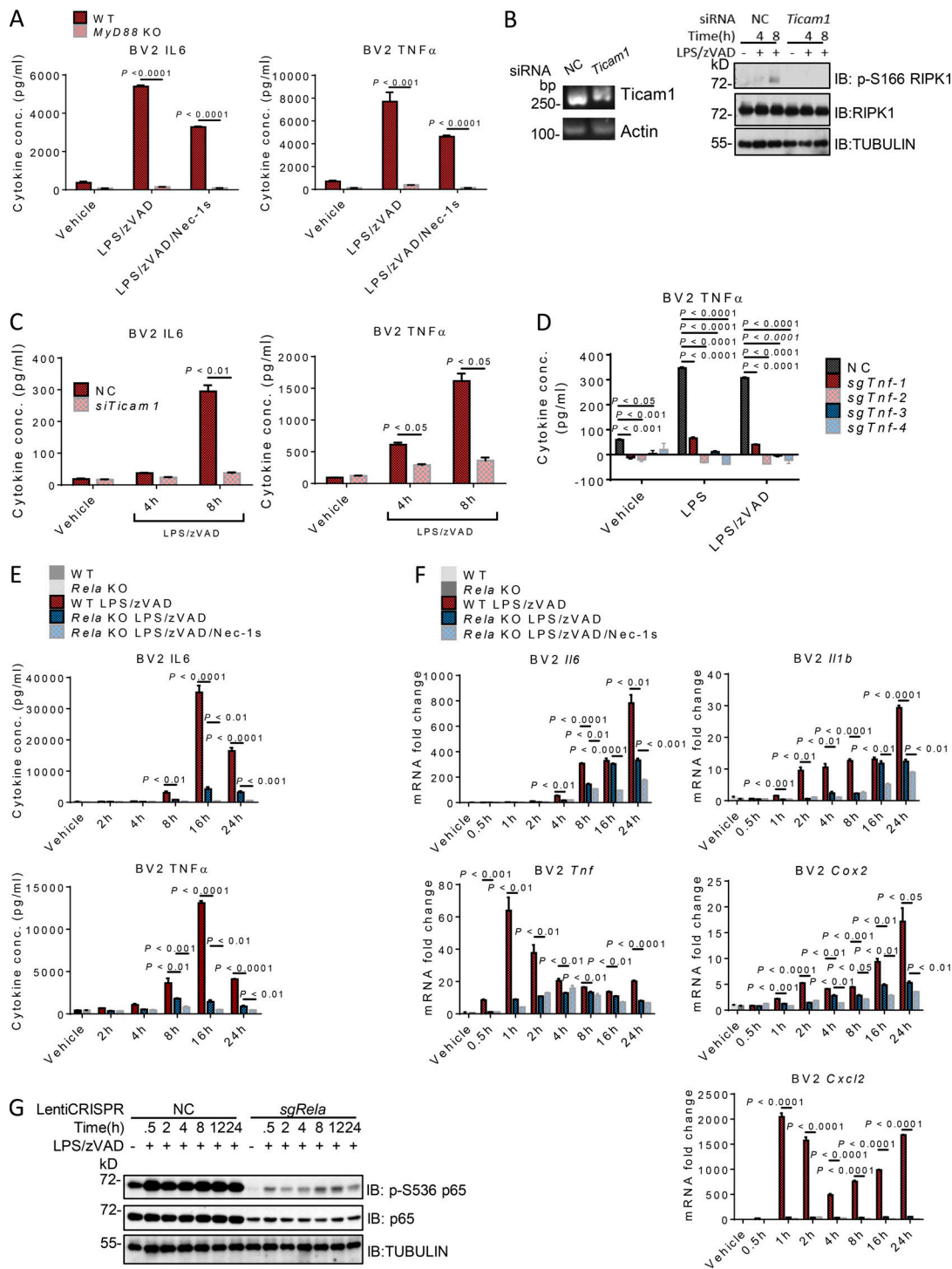


Figure S4. **LPS/zVAD-induced inflammation is mediated by Myd88, TRIF, and NF- κ B pathways.** (A) BV2 cells were treated as indicated for 8 h. The cell culture medium was collected and analyzed by ELISA for secretion of TNF α and IL6. The mean of three technical repeats is shown ($n = 3$), and the results are representative of two independent experiments. (B and C) BV2 cells were treated with siRNA against *Trif* and LPS/zVAD for the indicated periods of time, and the cell lysates were analyzed by Western blotting (IB) with the indicated antibodies (B). IL6 and TNF α secretion were measured by ELISA (C). The mean of two technical repeats is shown ($n = 2$), and the results are representative of three independent experiments. Knockdown efficiency of *Trif* in BV2 cells was determined by semiquantitative PCR (B). NC, non-targeted control. (D) Control and *Tnf*-KO BV2 cells were treated as indicated for 12 h. The cell culture medium was collected and analyzed by ELISA for secretion of TNF α to confirm KO efficiency. The mean of three technical repeats is shown ($n = 3$). (E and F) WT and RelA-KO (*sgRela*) BV2 cells were treated with LPS/zVAD and with or without Nec-1s for the indicated periods of time. The secretion of IL6 and TNF α in culture medium was determined by ELISA. The mean of two technical repeats is shown ($n = 2$), and the results are representative of two independent experiments (E). The transcription levels of the indicated cytokines were analyzed by RT-qPCR assay. The mean of three technical repeats is shown ($n = 2$), and the results are representative of two independent experiments (F). (G) BV2 cells were treated with LPS/zVAD for different periods of time. The reduced levels of p65 in *sgRela* BV2 cells were confirmed by Western blotting. LPS, 10 ng/ml; zVAD, 50 μ M; Nec-1s, 10 μ M. Data are shown as mean \pm SEM.

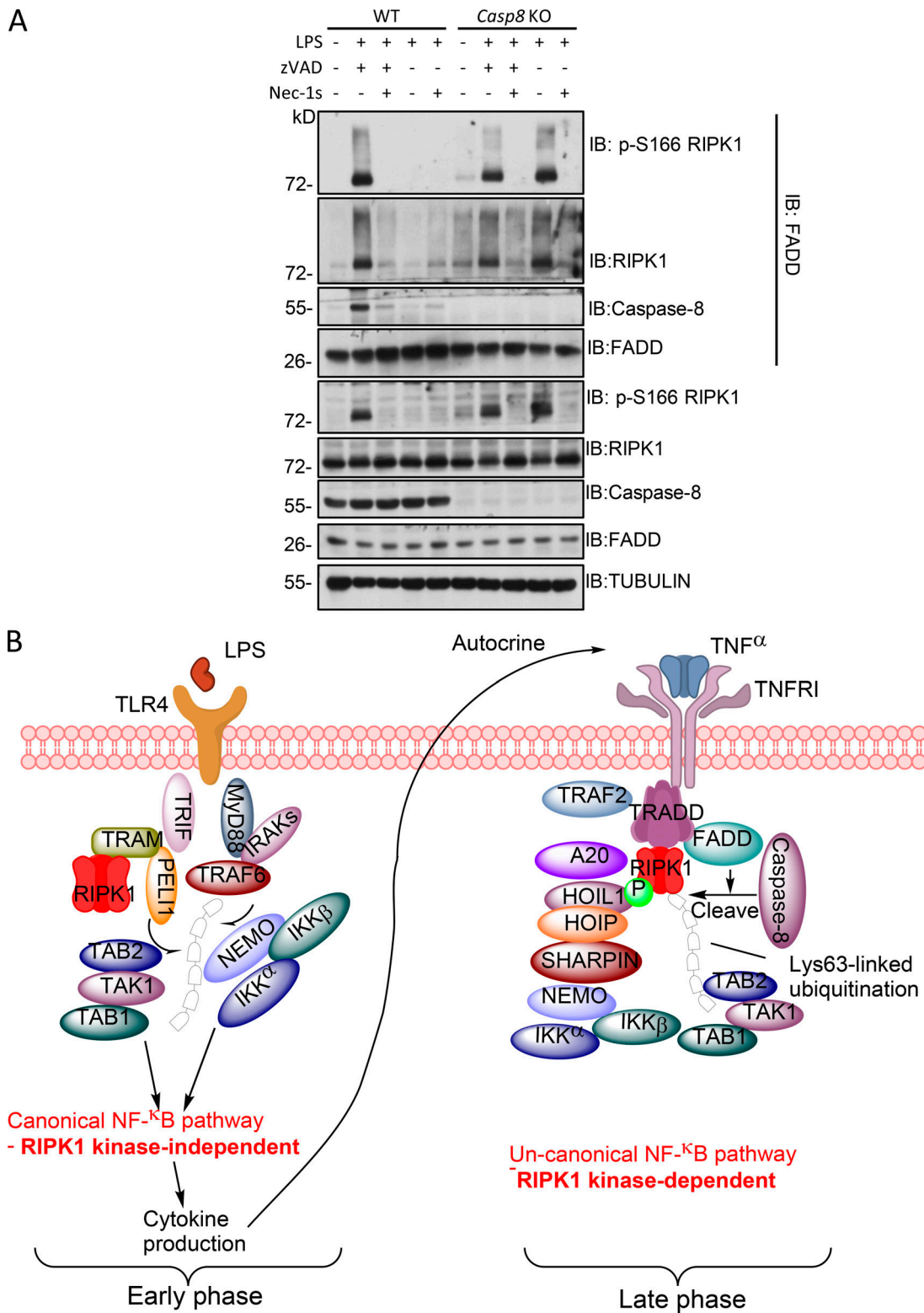


Figure S5. **A model for RIPK1 kinase to recruit NF- κ B mediators to promote sustained inflammation.** (A) WT and *Casp8*-KO BV2 cells were treated as indicated for 8 h, and cell lysates were immunoprecipitated with antibody against FADD. The immunoprecipitates and cell lysates were analyzed by Western blotting (IB) with the indicated antibodies. (B) A model of the NF- κ B pathway and cytokine production regulated by RIPK1 kinase activity in cells stimulated by LPS with caspase inhibition. LPS stimulation promotes the formation of an IKK complex and canonical NF- κ B signaling, which lead to the increased production of TNF α . When the enzymatic function of caspase-8 is inhibited, autocrine production of TNF α activates TNFR1, which leads to the formation of another complex, including the components of complex II, FADD, cFLIP, caspase-8, and RIPK1. This complex interacts with the canonical NF- κ B mediators, such as HOIP, SHARPIN, TAK1, TAB1/2, and IKK α / β , to mediate the RIPK1 kinase-dependent uncanonical NF- κ B pathway to promote the sustained production of proinflammatory cytokines that can be inhibited by the RIPK1 kinase inhibitor.

Provided online is one table. Table S1 lists peptides of the proteins interacting with activated RIPK1 identified by mass spectrometry.